

RSC Advances



This is an *Accepted Manuscript*, which has been through the Royal Society of Chemistry peer review process and has been accepted for publication.

Accepted Manuscripts are published online shortly after acceptance, before technical editing, formatting and proof reading. Using this free service, authors can make their results available to the community, in citable form, before we publish the edited article. This *Accepted Manuscript* will be replaced by the edited, formatted and paginated article as soon as this is available.

You can find more information about *Accepted Manuscripts* in the [Information for Authors](#).

Please note that technical editing may introduce minor changes to the text and/or graphics, which may alter content. The journal's standard [Terms & Conditions](#) and the [Ethical guidelines](#) still apply. In no event shall the Royal Society of Chemistry be held responsible for any errors or omissions in this *Accepted Manuscript* or any consequences arising from the use of any information it contains.



Journal Name

ARTICLE

Green solvents ionic liquids: structural directing pioneers for microwave assisted synthesis of controlled MgO nanostructures

Arvind H. Jadhav, Alan C. Lim, Gaurav M. Thorat, Harsharaj S. Jadhav, and Jeong Gil Seo*

Received 00th January 20xx,
Accepted 00th January 20xx

DOI: 10.1039/x0xx00000x

www.rsc.org/

Magnesium oxide (MgO) is one of the auspicious metal oxide which fascinated much attention because of its superior performance in scientific applications. Controlled facial arrangement of MgO nanostructures with tailored property is highly important in nanotechnology and nanoscience. Here, various MgO nanostructures were obtained via one pot microwave (MW) assisted synthesis in various structural directing ionic liquids (ILs). These selected ILs are based on mono cationic and dicationic moieties which consists of *N*-methyl imidazolium and 3-methyl pyridinium cations with various halide anions. Different designer solvents with respect to their counter anions produced various nanostructures, varying from nanoflakes, interconnected nanoparticles, hexagonal nanoparticles, irregular nanoparticles and nanocapsules, respectively. In this method, green solvents ILs are not only acting as solvent but also acting as structural directing agents. In addition, plausible mechanism of nanomaterial formation under MW irradiation in presence of ILs was also determined. Formation of hydrogen bonding with favorable π - π interactions by simply tailoring ILs structures by means of MW condition is the key factor for the development of different morphology. To define catalytic activity of prepared nanostructures, Claisen condensation reaction was performed. Results showed that, all nanostructures have efficient catalytic activity due to tailored structure, basicity, and surface area. Particularly, catalytic amount of hexagonal MgO morphology obtained from dicationic [C₄(mIm)₂Cl₂] IL showed 100 % conversion and 95 % remarkable selective yield of respective product. Proposed approach for nanomaterial preparation do not requires additional template and harsh reaction condition which establish a simple method to reduce the cost of production using environmentally benign solvents.

1. Introduction

Nanostructure metal oxides have recently experienced considerable attention because of its wide spread and interesting applications which are due to their unique shape and size dependent properties.^{1,2} Especially, nano MgO has broad range of physicochemical properties and extremely noteworthy functional metal oxide for use in diverse scientific field.^{3,4} MgO is applied as functional material in super capacitor, conductor, additives, toxic waste remediation, cosmetics, and used as base in catalyzed reactions.³⁻⁶ In last few decades, enormous efforts have been paid to prepare various MgO morphologies with enhanced surface area and controlled properties. Several conventional methods have been used for synthesis of MgO morphologies such as thermal oxidation, soft template assisted growth, hydrothermal, solvothermal, spray pyrolysis, thermal evaporation, chemical vapour deposition, and precipitation techniques.⁷⁻¹¹ By using these methods different morphologies have been prepared varying from particles, rods, wires, belts, tubes, nanoflakes and etc.⁷⁻¹¹ In most popular template assisted methods, surfactants and polymers with suitable solvents are generally applied to stabilize surface of nano-nuclei. In this case kinetically regulate growth of metal oxide facets which further leads to development of nanostructure in well-define morphology.¹² However, including template assisted method all these process have certain disadvantages as they either use high temperature or high

pressure. Apart from this, template assisted process need expensive organic templates, surface capping agents, toxic organic solvents as well as crucial reaction set-ups. To get additional benefits from widely spread applications of MgO as nanomaterial for various purposes, it is essential to tailor their morphology, size, surface area as well as surface chemistry.^{4,5} In case of oxide materials mainly engineering and catalytic phenomenon take place over surface of engineered materials.⁵⁻⁶ Surface property, architecture, and chemistry of MgO materials are crucial factors which leads selective pathway through the course of morphology development. Therefore, improving and exploring a new technique to prepare morphologically controlled MgO is still inspiring issue in nanoscience. Synthesize new morphology or develop a suitable green, one pot, simple non-conventional method using green solvent which produces outstanding architecture with enhanced properties of MgO are still desirable topics.

Of the several approaches hired today for construction of nanomaterials, microwave (MW) irradiation is a non-classical energy source has become increasingly popular in the science field.¹³⁻¹⁵ This approach helps to eliminate complex and time consuming non green processes and requires minimum investment in equipment, since it can be performed in a domestic MW oven. Similarly, nowadays use of this method in nanomaterial preparation is also increased drastically.¹⁶ MW in-core flash heating in dramatically reducing overall processing time is the main benefit associated with this method. In addition, higher reaction rate, rapid volumetric uniform heating, and selective high yield of products are some secondary benefits of this processes.^{14,15} Transformation of electromagnetic radiation in to heat energy in MW heating is based on two main factors conduction and dipolar polarization

Department of Energy Science and Technology, Energy and Environment Fusion Technology Center, Myongji University, Myongji-ro 116, Cheoin-gu, Yongin-si, Gyeonggi-do 449-728, Republic of Korea.

*Corresponding author: E-mail - jgseo@mju.ac.kr (J.G. Seo); Fax: +82-31-336-6336

phenomenon.^{14,15} Absorption of MW by conduction mechanism is more effective and reaction medium must produce high dielectric constant and high polar nature for MW absorption.¹⁴ Indeed, polar solvents such as ILs are best candidates for adsorption of MW irradiation which leads to production of conductive and high polar nature for reaction media.¹⁷

ILs are generally salts accumulated with organic bulky cations and inorganic anions. Recently ILs have attracted much devotion as reaction medium or catalyst because of their exceptional properties. They have wide liquid range, negligible vapor pressure, good stability at high temperature and good dissolving ability with high ionic conductivity.¹⁸ The opportunity to vary cations and anions combination gives number of ways to enhance ILs properties.^{17,19,20} Additionally, being solvents ILs can also act as reactant or catalyst in reaction and template or designer agent in synthesis of inorganic materials.²¹⁻²⁴ In recent times, by combining these both advantages, ILs and MW heating there are very few methods which shows synthesis of inorganic materials.^{15,25} By using these approaches different morphologies of inorganic nanomaterials have been produced. Results of these methods shows, synergetic effect of ILs with MW irradiation obtained significant selective morphology, high yield in short reaction time. However, there is no report which could show different controlled MgO morphologies by means of MW irradiation in different ILs as designer solvents. Therefore, it is essential to study nonconventional technique which open the prospect of realizing fast synthesis of nanomaterials in green solvent system such as ILs which make process more faster, eco-friendly as well as cheap economically.

Herein, different perfect morphologies of MgO nanostructures were obtained in one-pot using MW irradiation process in numerous structural directing ILs. The synthesized well accumulated designer solvents such as monocationic and dicationic ILs with counter anions controlled various MgO morphologies. Aside from a variation of ILs structures, influences of various cations and anions on morphology development were also investigated. Results revealed that, ILs acted as solvent as well as structural directing agent in presence of MW irradiation. Obtained results of MW assisted synthesis were compared with other conventional methods. This work provides a versatile approach to synthesize various MgO crystals of different morphology by varying structural directing agents (ILs). Plausible mechanism for the formation of different morphology of MgO in ILs is also discovered. We show here that slight structural modification of ILs is highly responsible for achieve selective crystal growth in MW irradiation condition. In addition, catalytic activities of these morphologies were also determined.

2. Experimental

2.1. Materials: Magnesium acetate tetra hydrated ($\text{Mg}(\text{CH}_3\text{COO})\cdot 4\text{H}_2\text{O}$) (99 %), Sodium hydroxide (NaOH) (99 %) (Acros), *N*-methyl imidazole (99 %), chlorobutane (99.0 %), Dichlorobutane (99 %), 3-methyl pyridine (99 %), acetonitrile (99 %), ethyl acetate (HPLC grade), ethanol (reagent grade), Chloroform-d (CDCl_3) (99 %). Reagents were used as received without further purification. All solvents were purchased from commercial sources. Double-distilled water was used throughout experiments.

2.2. MgO nanostructures characterization methods: Crystal structures of MgO morphology were confirmed by using X-ray diffraction patterns and results were recorded on a Rigaku Miniflex (Japan) X-ray diffractometer using Ni filtered Cu $K\alpha$ radiation. FE-TEM analyses were implemented using a TECNAI-32F30 transmission electron microscope with an acceleration voltage of 200 kV. Morphology of nanostructures were monitored by using field emission scanning electron microscope (FE-SEM) (Carl Zeiss Sigma

VP FE-SEM). Brunauer-Emmett-Teller (BET) surface areas of nanostructures were obtained from N_2 sorption isotherms acquired using a BEL Japan (Belsorp-II) instrument. Elemental composition and mapping of nanostructures were determined using an energy dispersive X-ray analyzer (EDS) coupled to SEM. FT-IR spectra of prepared nanostructures were recorded on a Varian 2000 IR spectro photometer by using KBr disc method. Thermogravimetric analysis (TGA) were accomplished on Scinco TGA *N*-100 instrument with heating rate $5^\circ\text{C}/\text{min}$ in a nitrogen atmosphere. UV-visible spectra were achieved on Varian Cary (100 Conc.) using bauble distilled water as standard. Raman spectra were obtained using LabRam HR800 UV Raman microscope (Horiba Jobin-Yvon, France) Spectrometer using focal length 80 and CCD detection at room temperature. Photo luminescence analyses of nanostructure were performed on Princeton Instrument Co., IRY1024, USA, using He-Cd 325 nm laser and ICCD detector at room temperature. CO_2 TPD measurements were carried out using BELCAT-A (BEL Japan, Inc.).

2.3. Preparation of designer solvents monocationic and dicationic ILs : Detail synthesis procedure and characterization data of all ILs are described in supporting information.

2.4. Preparation of MW assisted MgO nanostructures in ILs : For preparation of various MgO morphologies, initially, ILs were dried in vacuum oven at 70°C for 12 h and utilized it for further process. 2.2 g of $\text{Mg}(\text{CH}_3\text{COO})_2\cdot 4\text{H}_2\text{O}$ as precursor was added in 5.0 g specific IL in a 50ml Pyrex glass flask. Sufficient amount (1-2 g) of NaOH was added in reaction mixture. Mixture was stirred in presence of MW heating for 4-5 min. MW heating was repeated 6-7 times giving a break of 1-2 min at appropriate temperature. Cyclic mode was preferred in order to reduce risk of over heating or decomposition of ILs. MW operated under power radiations of 400 using a MW oven (DAEWOO model KOC-1B3KP, Korea). Reaction temperature was kept above melting point of ILs by adjusting temperature controller. After completion of MW heating cycles, mixture slowly cooled at room temperature. Addition of 20 ml double distilled water was done in reaction mixture and centrifuged at 8000 rpm for 20 min to remove aqueous layer. Obtained white slurry washed several times with double distilled water and centrifuged in order to remove IL from nanostructures. Finally, product was dried at 70°C for 12 h in a vacuum oven and calcined at 500°C for 5 h in presence of N_2 to obtained white solid powder. All different morphology development reactions were repeated 2-3 times using same reaction condition.

3. Results and discussion

Primary aim of this study is to access the conventional tailor-made ILs as structural directing agent for nanostructure development in assistance with MW irradiation. Our key concern is whether low melting point ILs are enough stable in flash MW heating while formation of morphology, since it is reported ILs are enough stable in conventional hydrothermal and other heating modes. In addition, literature reveals that, there were no substantial pressure created by ILs in reaction set-up in conventional mode which indicates convenient solvent for material preparation. For this process restricted number of ILs, such as, [Bmim] $[\text{BF}_4]$, [Bmim] $[\text{PF}_6]$, [Emim CO_2H] $[\text{BF}_4]$, and [Emim] $[\text{EtSO}_4]$, have been utilized in preparation of nanostructures by means of conventional technique.²⁶⁻²⁸ In last decade, consideration have paid to ILs contains BF_4 or PF_6 , which shows hydrophobic nature and releases poisonous and corrosive HF which do not follow standard of greener method.²⁶ Contrariwise, in present study, attention have paid to conventional hydrophilic ILs those are highly biodegradable, easily accessible and synthesized by greener method, which enhance possibility to use ILs

on large scale for development of nanostructures in both conventional and nonconventional methods.

3.1. Selection of ILs as designer agent for MgO nanostructures

Several reports confirmed that ILs can act as designer solvents or templates, and influence on physicochemical properties of nanostructures.^{18,29} Formation of morphology in materials can be attributed due to higher nucleation rate of nanostructures in ILs. To determine effect of components such as cationic and anionic moiety of ILs on nucleation and morphology formation, five different types of ILs were selected. These ILs have different combinations of organic bulky cations and inorganic anions. Fig. 1 covers five different ILs and their structural combinations.

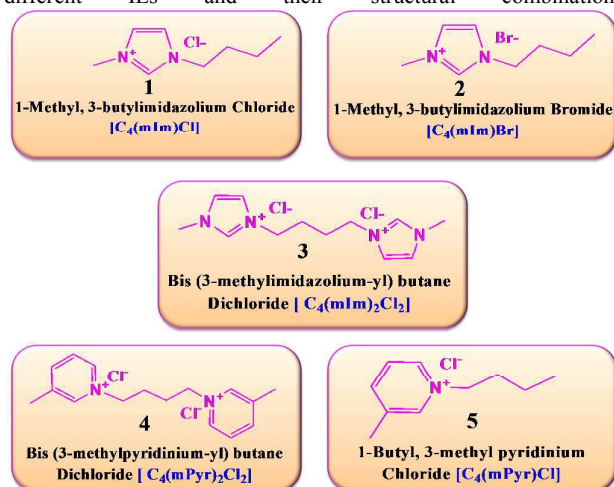
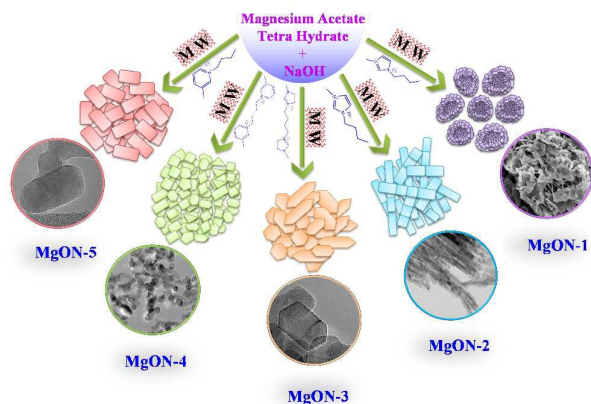


Fig. 1. Various monocationic and dicationic ILs used for preparation of controlled MgO nanostructures in presence of MW irradiation

Selection of traditional anions chloride (Cl⁻) and bromide (Br⁻) containing hydrophilic ILs can be produced easily using simple method. Previous studies reports that, coordination of these kinds of anions have direct impact on particle construction as well as morphology growth with respect to cations.²⁹ On the basis of structural features of ILs, organization of ILs can be tailored (cations and anions) and interaction energies of ILs can be modify.³⁰ On the other hand, MgO nanocrystals are composed of positively charged Mg layers and negatively charged O layers. Various different cationic and anionic structure of ILs possibly formed different interactions with MgO crystals which lead to development of different morphology. This factor is highly responsible for diverse mechanism, including formation of self assembly, hydrogen bonds, electrostatic attractions, and π - π stacking interaction.²⁹ Special constructed structure of ILs with respect to fascinating properties of large cations and anions of ILs convince to act as self-assembling template. Pre-organized solvent structure inspire nanocrystals to experience self-organization for development of well-defined nanostructures in presence of MW irradiation.²⁹ Different cations such as imidazolium and pyridinium were selected by considering following characteristics. Imidazolium-based ILs are among the most frequently used species because of their outstanding physicochemical properties and biodegradability.³⁰ Monocationic, butyl, methyl imidazolium [C₄mIm] contains with bulky organic moiety, which can contribute in π - π interactions and hydrogen bonding.²⁹ Attachment of butyl chain with aromatic ring is supposed to control agglomeration and size distribution of nanostructure dispersion. While, selection of same counter imidazolium dicationic core with short alkyl chain as spacer between two imidazolium cations possess two-fold π - π interactions and hydrogen bonding and enhanced other properties.¹⁹ Previous reports shows that, as

compared to monocationic ILs their dicationic counters ILs possess high thermal stability, polarity, and conductivity.^{19,30} Due to these enhanced properties in dicationic ILs which leads to develop different morphology and significant effects on MgO nanostructure. Other types of ILs were selected as pyridinium based monocationic and dicationic ILs with Cl⁻ as counter anions. These ILs does not have any characteristic acidic protons like imidazolium-based cations have but aromatic group with their effective interactions are still existent which could be elaborate in π - π interactions and can produce variation in morphology.²⁹ These five different types of ILs, showed significant influence on MgO nanostructure development. Obtained morphology of MgO in these ILs onwards designated as MgON-1, MgON-2, MgON-3, MgON-4, and MgON-5 as well as schematically represented in Scheme 1.



Scheme 1. Schematic representation of various controlled MgO morphology achieved from different ILs using MW irradiation

3.2. TGA and XRD analysis of MgO nanostructures

Fig.S-1 (supporting information) shows TGA analysis of as synthesized MgON-3 protocol with temperature growth from 25 to 850 °C. TGA results show that, initially weight remained constant until 350 °C, after that dropped rapidly. Sudden loss in weight was observed at around 350-425 °C, which correlates well with approximately 30 wt.%. This weight loss was corresponds to loss of hydroxyl molecules and some residual water as well as remain organic moieties by ILs in nanostructures. Above 425 °C temperature, there is no weight loss observed, showing that obtained resultant MgO material has admirable thermal stability at high temperature. Therefore, other successive synthesized samples were calcined at 500 °C for 5 h to obtain pure phase in morphologies achieved from various ILs. Obtained final morphology after calcination did not show any noticeable changes, original morphology is preserved after calcination in all prepared MgON. Few cracks/shrinkage were observed on nanostructures, possibly due to loss of hydroxide molecules or weight loss. However, morphology preserved topography and crystallinity throughout samples.

XRD peaks of calcined products of MgON acquired from different ILs are shown in Fig. 1. After annealing, all samples showed reflections corresponding to MgO as highly pure spinal phase. Diffraction peaks at 2θ values of 36.94 °, 42.80 °, 62.30 °, 74.67 °, and 78.61 ° were assigned to (111), (200), (220), (311), and (222) planes of cubic MgO nanoparticles. These obtained XRD patterns clearly confirmed presence of highly pure MgO cubic phase. Resulted diffraction peaks well matched with standard XRD pattern of MgO (JCPDS 45-0946) indicates formation of pure MgO compound in various ILs. MgON-1 produced in IL-1 showed highest intensity of diffraction peaks and followed by gradually decreases

with MgON-2, 3, 4, and 5, those are obtained from IL-2, 3, 4, and 5 respectively. However, intensities of all MgON nanostructures have comparable heights. Average particle sizes were calculated from peak width at half height by means of “Scherer equation” for MgON-1-5.³¹ Calculated average sizes were obtained in the range of 10-60nm, which is closely, resembles to their FE-SEM and FE-TEM images.

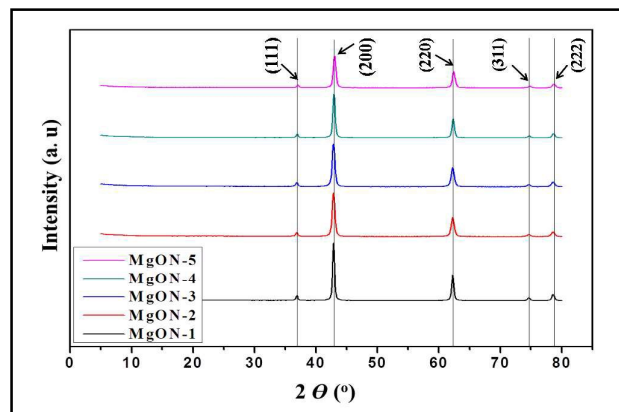


Fig.1. X-ray diffraction patterns of prepared MgON in different ILs

3.3. FE-SEM and FE-TEM analysis of prepared MgO nanostructures

All morphologies of MgON nanostructures were analyzed by FE-SEM and FE-TEM analysis. Fig. 2 illustrates FE-SEM, FE-TEM images and SAED pattern of MgON-1 sample which is obtained from monocationic IL $[C_4(mIm)Cl]$ at 90 °C. SEM images Fig. 2 (a, b) shows that imidazolium based monocationic ILs with Cl⁻ anions developed high quality “nanoflakes” like morphology throughout sample. Imidazolium cation of $[C_4(mIm)Cl]$ IL used in this technique might be interacted with precursor by hydrogen bonding and develop π - π interactions or electrostatic force and hydrogen bonding. $[C_4(mIm)Cl]$ IL has electron withdrawing ability by allocation of electron pair of hydrogen and carbon at place 2 of imidazole ring.^{29,32} These developed interactions pile-up and stack in presence of MW. Thus, $[C_4(mIm)Cl]$ IL was interacted with surface of developing MgO crystals which leads to anisotropic development of MgO crystals into nanoflakes.³² These obtained flakes structures in $[C_4(mIm)Cl]$ are approximately 50-70 nm in size and having 2-4 nm thickness. Surface of nanostructure flakes looks like rough and indicates that, it is composed of many primary building blocks formed by MgO nanoparticles.

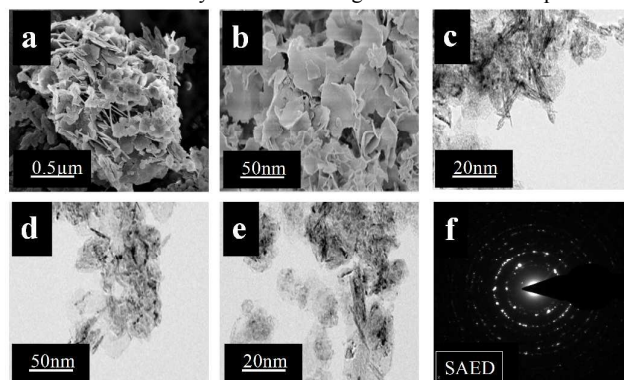


Fig.2. FE-SEM (a, b), FE-TEM (c, d, and e) images and SAED pattern (f) of MgON-1 nanoflakes obtained in $[C_4(mIm)Cl]$

These particles are dense and well interconnected with each other. Calcination does not showed any effect on shape and size of MgON-1 but some bangs and lines were observed. In calcination process H_2O molecules were lost between two adjacent layers and leads to periclase assembly with irregular inter crystallite networks which produce mesopores. These results can be also confirmed by FE-TEM images shown in Fig. 2 (c, d, and e). Some of these nanoflakes looks like fused with each other and transparent structures suggest that nanoflakes are very thin. Selected area electron diffraction pattern (SAED) of MgON-1 showed in Fig. 2 (f) indicates that, MgO nanoflakes are polycrystalline in nature. Single nanoflakes showed three noticeable diffraction rings consistent with XRD peaks, indicates formation of polycrystalline MgO with cubic structure.

Fig. 3 shows FE-SEM, FE-TEM, and SAED pattern of MgON-2 nanostructures obtained at 90 °C from monocationic IL $[C_4(mIm)Br]$ which has bromide (Br⁻) as an anionic moiety. From FE-SEM images (Fig. 3 (a, b, and c)) it can be clearly seen that, monocationic $[C_4(mIm)Br]$ IL successfully achieved different morphology than IL $[C_4(mIm)Cl]$ produced. We believed that, approximately similar type of mechanism and interactions were formed with $[C_4(mIm)Br]$ in presence of MW irradiation. Except, larger inorganic cation (Br⁻) with alkyl chain is responsible for producing variation in morphology. $[C_4(mIm)Br]$ IL produced “interconnected capsules” morphologies having 20-50 nm in length and 20-25 nm in width. These capsules are formed by combination of MgO nanoparticles as a building block element. After calcination surface of nanocapsules became rough and develop mesopores due to evaporation of hydroxyl molecules. In addition, Fig. 3 (d and e) shows FE-TEM images of representative interconnected nanocapsules which further support results obtained by SEM images. Clear pictures of finger like projections due to interconnected nanocapsules are seen very clearly in TEM images. SAED image pattern of morphology is displayed in Fig. 3 (f), which represents nanocapsules are well-crystallized poly crystals which gives strong agreement with XRD pattern of MgON-2 by showing characteristic three circular rings.

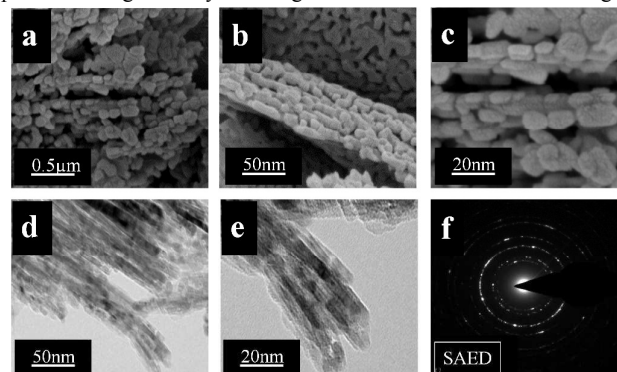


Fig.3. FE-SEM (a, b, and c), FE-TEM (d and e) images and SAED pattern (f) of MgON-2 interconnected nanocapsules obtained in $[C_4(mIm)Br]$

Another dicationic type of $[C_4(mIm)_2Cl_2]$ IL was applied for construction of MgO nanomorphology in MW irradiation at 90 °C. In this case, organic imidazolium based bulky dicationic and inorganic chloride dianions were used. These di-ions are separated by butyl alkyl chain bridging moiety. By using $[C_4(mIm)_2Cl_2]$ hexagonal disk like structures were developed. Compared with other ILs, obtained hexagonal MgO morphology in dicationic hydrophilic $[C_4(mIm)_2Cl_2]$ found very small in size. High viscosity of $[C_4(mIm)_2Cl_2]$ is key to develop such a small shaped hexagonal disc like structures. High nucleation rate and two-fold property as well as interactions in $[C_4(mIm)_2Cl_2]$ produced such an marvelous

morphology. It is reported that, in dicationic ILs, acidity as well as hydrogen bonding and their interactions were two fold compared to monocationic ILs. In case $[C_4(mIm)_2Cl_2]$ IL imidazolium dications showed major impact in hexagonal morphology. Imidazolium cations with smaller alkyl chains between these rings associated with Cl^- anions obstructs growth of nanostructures to develop in hexagonal shape due to steric hindrance effect. In addition, developed two-fold acidity, hydrogen bonding, and $\pi-\pi$ interactions are some other cause for fabrication of hexagonal morphology.²⁹ Fig. 4 (a, b, and c) represent FE-SEM images of calcined sample of MgON-3. Results reveal high quality hexagonal morphology developed throughout sample. Hexagonal structures are 40-60 nm in range and 10-20 nm thickness, which is consistent with result calculated from "Scherrer" equation. In addition, to determine the effect of increased time and reaction temperature on hexagon morphology, same reaction was conducted in twofold reaction time (10-11 MW cycles of 4-5 min duration) and increased temperature (150 °C) showed overgrowth in hexagons (Fig. S-2). Above increasing the reaction temperature of 150 °C resulted in decomposition in IL structure in MW condition.

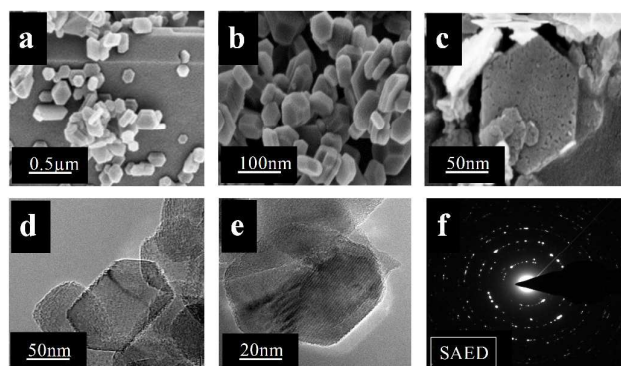


Fig. 4. FE-SEM (a, b, and c), FE-TEM images (d, and e), and SAED pattern (f) of MgON-3 nanohexagons obtained in $[C_4(mIm)_2Cl_2]$

Moreover, hexagons were composed of MgO nanoparticles. After calcination mesopores and some cracks were produced in hexagons due to water evaluation. However, morphology was same before and after calcination. Fig. 4 (d and e) shows FE-TEM images of hexagons. MgON-3 show perfect hexagonal structure with transparent nature. Transparent nature of hexagons indicates that, these nanostructures are very thin and porous. It can clearly observe in TEM images, hexagons are composed of granular MgO nanoparticles. Edges of hexagons are approximately equal in nature. SAED pattern showed in Fig. 4 (f) indicates that nanohexagons are polycrystalline in nature and these results are in line with XRD pattern of MgON-3. Furthermore, another group of ILs monocationic pyridinium based ILs $[C_4(mPy)_2Cl_2]$, which has chloride (Cl^-) as anion were applied for development of morphology in MW irradiation. Results of these observations fail to give any selective morphology with $[C_4(mPy)_2Cl_2]$, IL in MW irradiation.

Fig. 5 (a, b) illustrate FE-SEM images of MgON-4 nanostructure. In which, could not find any specific morphology. Circular nanoparticles, capsules, hexagonal structure, trigonal morphology as well as nanoplates were observed throughout sample 120 °C. IL $[C_4(mPy)_2Cl_2]$ composed of methyl group at subsidiary chain of pyridinium cations with Cl^- anions separated by butyl bridging moiety. Dicationic $[C_4(mPy)_2Cl_2]$ IL does not have any acidic proton and it fails to make efficient Hydrogen bonding with precursor.¹⁸ Interaction between formed MgO nuclei and ILs are too weak that could not serve effectively for nucleation and growth of morphology.^{19,29} Simple weaker $\pi-\pi$ interactions are present due to

pyridinium anions for development of morphology. In addition, these interactions are not flexible due to dicationic nature of ILs. Therefore, it fails to develop selective morphology under MW irradiation. Obtained morphologies are in range of 40-50 nm in size. Calcination does not show any effect and persevered original morphology after calcination. Some cracks and wounds were observed on these morphologies by formation of mesopores in annealing treatment. FE-TEM (Fig. 5 (c, d, and e)) images were also support to FE-SEM analysis. TEM images of MgON-4 shows nanodisks, trigonal structures, particles and capsules throughout sample. Size of nanostructures is in 40-50 nm having 10-20 nm thickness. Bumpy surface of nanostructure indicates it is composed of many primary MgO nanoparticles. SAED pattern (Fig. 5 (f)) obtained by focusing electron beam on an individual nanostructure showed poly crystalline nature with a face-centered cubic structure.

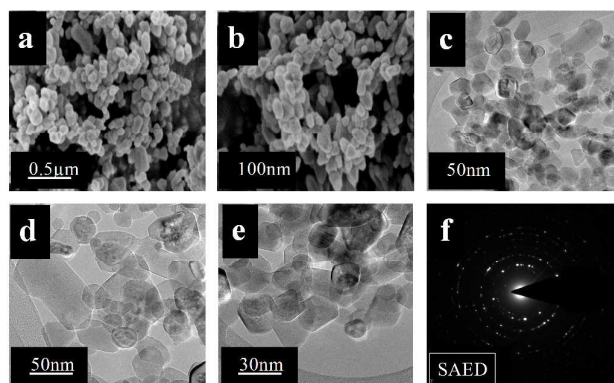


Fig. 5. FE-SEM (a, b), FE-TEM images (c, d, and e) SAED pattern (f), of MgON-4 irregular nanostructures obtained in $[C_4(mPy)_2Cl_2]$

FE-SEM images of MgON-5 are shown in Fig. 6 (a, b, and c) these nanostructures were fabricated in pyridinium based monocationic IL $[C_4(mPy)Cl]$ composed of pyridinium cations with Cl^- anion 90 °C. This pyridinium based ILs produced nanocapsules morphology of MgO. Specialty of this IL is, it does not have any acidic proton but have many flexible $\pi-\pi$ interactions between IL molecules and precursor.^{29,32} Butyl alkyl chain with pyridinium cation produce $\pi-\pi$ interactions and allow MgO crystal grow in a longer fashion which leads to formation of nanocapsules. Due to absence of acidic proton less hydrogen bonding produced and simple flexible $\pi-\pi$ interactions are responsible for morphology development.^{29,32} From obtained SEM results, it is observed that, after calcination parental morphology was remained in sample.

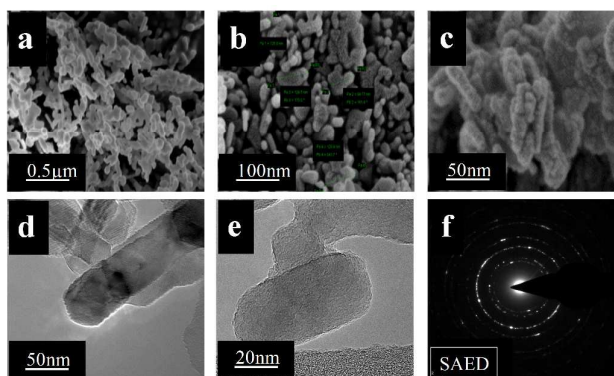


Fig. 6. FE-SEM (a, b, and c), FE-TEM images (d, and e), and SAED pattern (f) of MgON-5 nanocapsules obtained in $[C_4(mPy)Cl]$

However, some pops and lines are observed compared with as synthesized precursor due to H₂O evaporation during sintering which leads to formation of mesopores. Nanocapsules are 50-60 nm in length with 10-20 nm in width. FE-TEM images in Fig. 6 (d, and e) were also support to SEM analysis, it can be clearly seen that MgO nanocapsules is composed of nanoparticles. SAED patterns of calcined materials (Fig. 6 (f)) show circled rings, an indication of polycrystalline nature of sample which is in good agreement with XRD analysis of MgON-5.

3.4. Fourier transforms infrared (FT-IR) and Raman spectroscopic analysis of MgO nanostructures

Fig. 7 (a) demonstrates FT-IR spectra of MgON nanostructures obtained in this study. It is well acknowledged that MgO chemisorbs carbon dioxide and water molecules from the atmosphere due to its surface basic properties.³³ However, upon calcination of MgON at 500 °C, CO₂ and H₂O molecules elements and thus produce various Brønsted as well as Lewis acid and base sites on MgO surface. Main representative peak corresponds to Mg and O (Mg-O) stretching vibrations at 442 cm⁻¹ indication for formation of highly pure MgO.^{33,34} This characteristic peak was observed throughout all MgON samples synthesized in various ILs system. Occurrence of bands in calcined MgO at 1642, 1454, and 1029 cm⁻¹ are assigned to carbonate species, whereas weak absorption band at 2351 cm⁻¹ is ascribed to stretching vibrations of CO₂ due to physically adsorbed atmospheric CO₂.³³⁻³⁵ Band at 1082 cm⁻¹ is attributed due to H⁺ ion.³³ High intense absorption bands at 1634 and 3471 cm⁻¹ were attributed to OH bending and stretching vibrations correspondingly of physically adsorbed H₂O molecules as well as surface OH groups strongly disturbed by hydrogen bonding.³³⁻³⁶ These all different kinds of intense FT-IR peaks were also observed in every spectrum of MgON.

Furthermore, micro crystalline natures of morphologically controlled MgON nanostructures were also studied by using Raman spectroscopic. Fig. 7 (b) shows representative room temperature Raman spectrum of different MgO nanostructures. Results indicate presence of characteristic highly intense bands at 290 and 448 cm⁻¹ in prepared all MgON nanostructures. Raman intense peak at 448 cm⁻¹ may resemble with two projecting peaks in Chen's methodology in corresponds with MgO micro crystalline structure.^{37,38} Consequently, it is hypothetical that 290 cm⁻¹ peak is accompanying with a "TA" (Transverse acoustic) phonon" at micro crystalline nanostructure boundary, whereas 448 cm⁻¹ line with a "TO" (Transverse optic) phonon at microcrystalline nanostructure center.³⁸ Observed experimental Raman peaks are closely resembles with previously reported results. Additionally, observed peaks in

Raman spectrum validate presence of nanocrystalline phase, whereas such peaks are generally absent in bulk MgO materials.

3.5. Photoluminance and UV-Vis spectroscopy study of MgON nanostructures

Fig. S-3 shows typical photo luminescence (PL) spectra scanned at room temperature of MgON nanostructures. Oxygen vacancies or deficiencies in metal oxide surface act as an invisible enhancer in engineering purposes or in catalytic applications which significantly alter oxide properties.³⁹ Therefore, to determine oxygen vacancies in nanostructures developed at the time of construction is highly significant. Having a wide-band gap material, bulk MgO normally does not demonstrate PL activity at room temperature.⁴⁰ Earlier studies on PL of MgO nanostructures showed, intense peak at around 450 nm due to presence of oxygen vacancies on MgO.⁴¹ Presence of oxygen vacancies on surface of nanostructures is due to in-core MW heating preparation method or at calcination of magnesium hydroxide into MgO resulted into incomplete oxidation process. Due to these reason nanostructure may show emission in PL.^{41,42} In addition, defects associated with oxygen vacancies and Mg vacancies which leads to creation of new defect levels in band gap section of MgO structures and these defect states freely contribute in luminescence.³⁹⁻⁴² Obtained results illustrate presence of a strong intense peak at nearly 450 nm in all prepared MgON morphologies. At 450 nm some of MgON showed increased PL emission spectra. This considerable increase in PL emission in some MgON can be explained by transfer of photo generated carriers and optical resonant cavity development.^{41,42} Upon laser irradiation for PL measurement, photo generation, transfer, and recombination of carriers occur consecutively in core of MgON nanostructures. Some of these photo-generated electrons and holes recombine in MgO cores to emit light and enhances PL light.^{43,44} Hence, existence of PL emission in MgON nanostructures is due to presence of defects of oxygen vacancies on surface of MgON. These tailored oxygen vacancies are obtained because of ionic media used at the time of construction of nanostructures by mean of MW irradiation.

Fig. S-4 shows UV-vis spectra of MgON nanostructures. Intense peaks were found at 278 nm and 296 nm, which can be attributed due to excitation of electrons present at four coordinated anions on edges and three coordinated surface anions on corners as exhibited in crystal structure of MgO in Fig. S-5.⁴⁵ Calculated band gap value from UV-vis spectra was 4.3 eV and results are displayed in Fig. S-6. Lower band gaps of MgON nanostructures are due to occurrence of anions which is four co-ordinated at surface of edges in MgON, while bulk material holds a band gap of 7.8 eV due to existence of six coordinated surface anions.⁴⁵

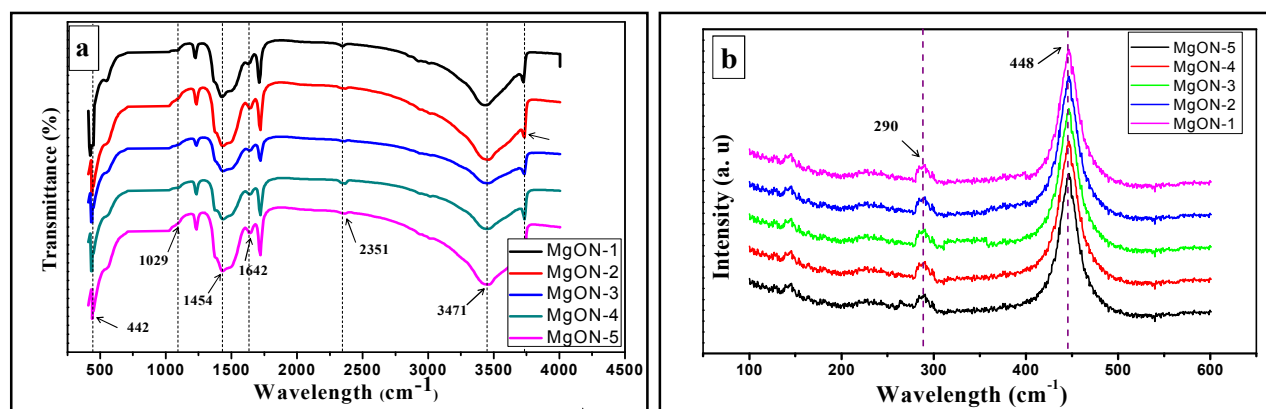


Fig.7. (a) FT-IR analysis, and (b) Raman spectroscopy analysis of different MgO nanostructures prepared in ILs

3.6. Energy-dispersive spectroscopy (EDS) analysis of MgO nanostructures

Fig. S-7 displays EDS spectra as well as EDS mapping of prepared MgON. EDS spectra revealed that, synthesized products are principally made of purely Mg and O with an atomic proportion ratio of 1:1 correspondingly. These EDS results are well consistent with XRD results and it is exposes that there is no any other impurity were observed in samples by EDS as well as XRD. Slight lower amount of oxygen indicates, due to presence of oxygen deficiency in MgON nanostructures, which might have been developed during rapid establishment of MgO crystals under MW irradiation. These oxygen deficiency occurrence already proved by PL spectroscopy.

3.7. BET and pore analysis of MgO nanostructures

Additionally, to examine effect of different ILs on texture property and effect on pores of MgON nanostructures, BET and pore analysis were performed. Surface area, pore diameter, pore volume, as well as basicity of all nanostructures prepared in various ILs are summarized in Table 1. N₂ adsorption-desorption isotherms of synthesized different MgON are shown in Fig. 8 (a, b, c, d, and e). BET surface area of these structures is in range of 50-75 m²/g. From these obtained isotherms shows that all MgON morphology reveals characteristic "Type-III" isotherms with BET surface areas of 48.15, 56.23, 74.31, 49.61, and 61.27 m²/g for MgON-1, 2, 3, 4, and 5, respectively. In comparison of BET surface area with MgO prepared in different ILs by means of MW irradiation method is larger than that of the conventional methods. Obtained results of surface area reveals that, MgON-3 and MgON-5 which was synthesized in dicationic imidazolium and pyridinium based ILs have higher surface area compared to MgON synthesized in monocationic ILs. On other side, chloride anion containing both cationic moieties reveals approximately similar surface area. Br⁻ anion containing imidazolium based monocationic ILs showed 56.23 g/m² surface area. From these obtained results, it can conclude that, different ILs media showed strong influence on surface area of MgON prepared by means of MW irradiation method.

Table 1. Surface area determination and texture properties of synthesized different MgON.

Nano structure	Morphology	Surface area (m ² /g)	Total pore volume (cm ³ /g)	Average pore diameter (nm)	Basicity* (mmol/g)
MgON-1	Nanoflakes	48.2	0.49	24.2	0.73
MgON-2	Interconnected nanocapsules	61.2	0.91	31.6	0.86
MgON-3	Hexagonal nanostructures	74.3	0.82	26.6	1.68
MgON-4	Irregular nano particles	49.6	0.69	36.2	1.32
MgON-5	Nanocapsules	56.2	0.88	25.5	0.92

*Total basicity determined by CO₂ TPD

Porosity of nanostructures is an important physical property of materials which is strongly effect on adsorption properties, catalytic activity, toughness, permeability, material mechanical strength, and etc. Pore size distributions of these materials are revealed in Fig. 8 (f). Isotherms acquired for MgON nanostructures indicates, pores in all MgON are belong to mesopores category and size range of mesopores found in between 5-35 nm. Pore volume of MgON did not showed any trend with respect to different ILs used in preparation methods. Average pore diameter of MgON showed in 0.50-1.0 cm³/g range. From these observations it can conclude that, surface area and pore volume of MgON nanostructures affected by both cations as well as anions present in ILs. In addition, basicity of MgON were also determined by CO₂ TPD method. Results reveal that basicity was also affected tremendously with respectively different ILs. Total basicity was found in range of 0.75-1.70 mmol/g. However detail investigation of effect of different ILs on basicity is in under process.

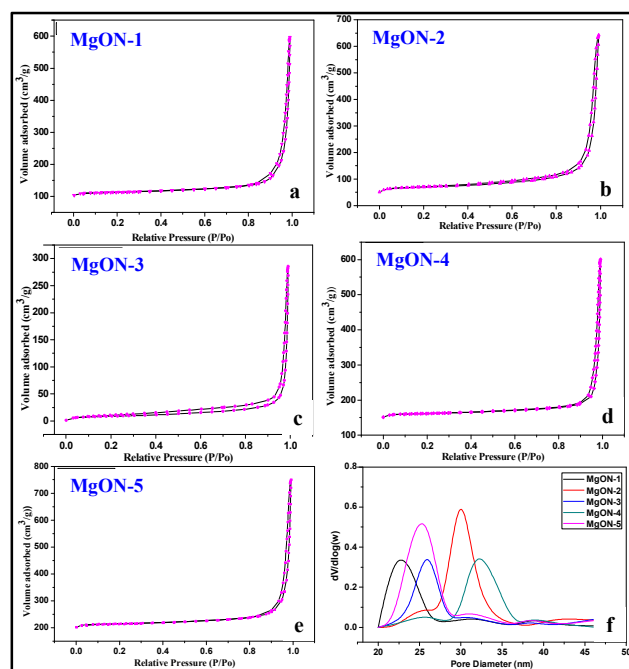


Fig. 8. N₂ adsorption-desorption isotherms of MgO nanostructures prepared in ILs (a-e) pore diameters of various morphologies of MgO (f).

3.8. Proposed mechanism

MW assisted synthesis of nanostructures is non-conventional method which enhances rapid homogeneous heating in contrast to conventional heat-assisted method. To evaluate benefit of MW assisted nanostructures syntheses in ILs, results were compared with conventional hydrothermal as well as oil bath heating methods those are famous conventional synthesis method. To clarify the mechanism of current reaction in ILs, following control reactions were performed. Mg(CH₃COO)₂•4H₂O with NaOH were dissolved

in respective IL at 120 °C using conventional heating method and reaction was repeated under identical conditions including all ILs used in this report. Products as MgO nanopowder without any morphology were isolated in all cases after calcination. Furthermore, Mg (CH₃COO)₂·4H₂O was dissolved in water with NaOH and stirred at 120 °C, meanwhile reaction was also performed under same condition in a MW oven. There were no any specific morphology in product were obtained in these reactions. Furthermore, ethylene glycol as solvent was used, because of polarity, high viscosity and high thermal stability. This reaction was conducted at 150 °C reaction temperature, as well as same reaction was also performed in a MW oven at 150 °C. Results of these reactions were also fails to give any specific morphology in products. These same reactions were also conducted in reflux temperature of ethylene glycol and same condition was maintained up to 5 h. As a result MgO powder was obtained at the end as product without any morphology. Hence, to control morphology of MgO nanostructures, specific ionic media as well as in core heating is necessary to obtain selective structures, which can be provide by means of MW irradiation in ILs media. Therefore, by using simple non-conventional MW heating achieved highly selective nanostructures of MgO morphology throughout samples in respective ILs media. These observations states that, specific ionic environment with MW irradiation is highly responsible for formation of MgO morphology.

In addition, functional aspect of reaction media (ILs) in reaction system of nanoparticle synthesis is to control rate of nucleation and growth of particles, like surfactant acts in conventional methods.³¹ Especially, different interactions between ILs and metal oxide structure developed at the time of morphology construction in presence of MW irradiation which leads to plausible mechanism for development of various morphology. Fig.9 shows possible interactions between ILs and metal oxide particles. In continuation with discussion, on the basis of nature and structure of IL, interactions between ILs and metal oxide can be develop and varies.²⁹⁻³¹

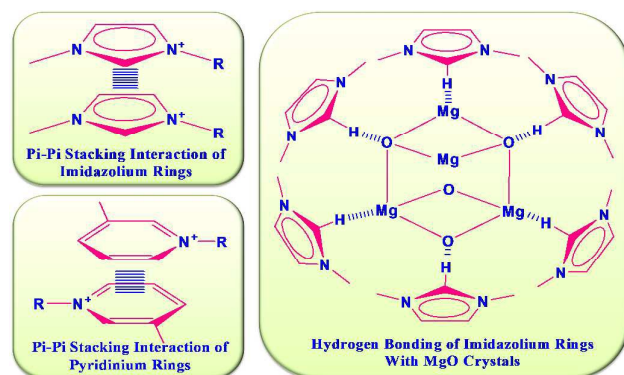


Fig.9. Schematic representation of interactions between ILs with MgO crystals in presence of MW irradiation.

Aromatic moiety of ILs can contribute in π - π interactions. It deals as a highly electron accepting section and it is also probably responsible for electrostatic attraction with surface of metal particles having polar moieties.²⁹ Acidic proton present in between two nitrogen atoms of imidazolium ring structure can act as a bridging moiety at the time of formation of hydrogen bonding. It is also reported that, both electrostatic and coordination effect of imidazolium cations contribute in nanoparticle morphology stabilization in presence of ILs.^{29,32} Depending on different ILs with different components of cations with respective to anions, different interactions including electrostatic attraction, π - π stacking interaction and hydrogen bonds, as well as self-assembly can be expected to occur between ILs and precursor. These interactions of

reaction components lead to MgO unit growth projecting to development rate in specific morphology.³²

While performing reaction in MW irradiation condition, MW irradiation also plays very vital role in nanostructure construction. MW irradiation support efficient internal “in core” heating and reaction temperature raised consistently throughout whole ILs media by direct accepting of MW energy to molecules that are present in reaction mixture.²⁹ MW irradiation triggers heating by two main factors, namely dipolar polarization and another ionic conduction.⁴⁶ Whereas, dipoles in reaction mixture produced by ILs are created dipolar polarization effect as well as contribute in ionic conduction. When exposed to MW irradiation, dipoles in reaction mixture align in the direction of applied electric field (Fig.10). As electric field oscillates, molecular dipoles accordingly attempt to re-align themselves along the alternating electric-field restructures and in such process energy is vanished in form of heat through molecular collisions.^{46,47} Amount of heat released by this course is directly associated to ability of dipoles to align with frequency of applied field.⁴⁷ If dipole does not have sufficient time to rearrange or reorient too quickly with applied field, no heating will occur at molecular level.^{29,46-51} We believed that, at this stage of morphology development conventional heating methods fails to supply applied field at molecular level.

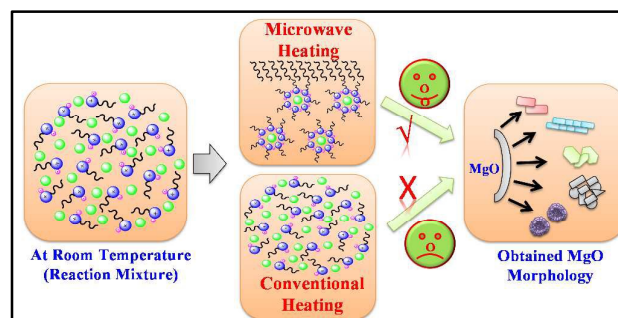


Fig.10. Plausible mechanism and schematic representation of formation of MgO nanostructures in ILs using MW irradiation

Whereas “in core” flash heating raised steadily throughout whole ILs media. This is the main cause for formation of obtained MgO nanostructures by means of MW irradiation in ILs. Moreover our experimental results also verified this hypothesis by comparison of conventional and microwave heating experimental results for MgO morphology development in various other solvents.

3.9. Catalytic Activity of MgON

To determine catalytic activity of prepared morphologically controlled MgO nanostructures “Claisen condensation reaction” was performed. This reaction mainly based on basic property of catalyst and active centers present in catalyst. As compared to pure MgO, synthesized MgO in this study showed highly tailored basicity by CO₂ TPD (Table 1). Therefore, this reaction gives focus on tailored basicity which altered due to their preparation method using MW irradiation in various ILs. Table 2 demonstrates results of synthesis of chalcones by using Claisen condensation reaction of acetophenone (1) and benzaldehyde (2) as model compounds using catalytic amount of MgO nanostructures. Initially, catalyst free reaction of 1 and 2 in ethanol at 120 °C temperature was performed which did not show any product after 72 h (Entry 1). To determine activity of prepared MgON as catalyst, numbers of reactions were performed at same condition in ethanol. Prepared different all catalyst were tested for this reaction using 0.1 equiv. catalyst amount and discovered remarkable catalyst among prepared MgON (Entries 2-6). Results show that, all performed reactions with MgON were carried very well and provide good to excellent yield of product (up-

32. R.R. Gandhi, S. Gowri, J. Suresh, M. Sundrarajan, *J. Mater. Sci. Technol.*, 2013, **29**(6), 533.
33. N.C.S. Selvam, R. Thinesh Kumar, L.J. Kennedy, J.J. Vijaya, *J. Alloys Compd.* 2011, **509**, 9809.
34. J. Zhou, S. Yang, J. Yu, *Colloids Surf.A*, 2011, **379**, 102.
35. H. Niu, Q. Yang, K. Tang, Y. Xie, *J. Nanopart. Res.* 2006, **8**, 881.
36. J. Xu, Y. Ao, D. Fu, C. Yuan, *Appl. Surf. Sci.* 2008, **255**, 2365.
37. H. Ding, K.T. Yong, I. Roy, H.E. Pudavar, W.C. Law, E.J. Bergey, P.N. Prasad, *J. Phys. Chem. C*, 2007, **111**, 12552.
38. L. Bertinetti, C. Drouet, C. Combes, C. Rey, A. Tampieri, S. Coluccia, G. Martra, *Langmuir*, 2009, **25**, 5647.
39. G. Pacchioni, *ChemPhysChem*, 2003, **4**, 1041.
40. S. Xie, X. Han, Q. Kuang, Y. Zhao, Z. Xie and L. Zheng, *J. Mater. Chem.*, 2011, **21**, 7263.
41. L. Kumari, W.Z. Li, C.H. Vannoy, R.M. Leblanc, D.Z. Wang, *Ceram. Interfaces*, 2009, **35**, 3355.
42. B.M. Maoz, E. Tirosh, M.B. Sadan, I. Popov, Y. Rosenberg, G. Markovich, *J. Mater. Chem.*, 2011, **21**, 9532.
43. H.S. Kim, H.W. Kim, *Acta Phys. Pol., A*, 2009, **116**, 58.
44. K. Ishikawa, N. Fujima, H. Komura, *J. Appl. Phys.*, 1985, **57**, 973.
45. M. Sterrer, O. Diwald, E. Knozinger, *J. Phys. Chem. B*, 2000, **104**, 3601.
46. C.O. Kappe, A. Stadler, *Microwaves in organic and medicinal chemistry*; Wiley-VCH: Weinheim, 2005.
47. K. Richter, P.S. Campbell, T. Baecker, A.S. Itzek, D. Yaprak, A.V. Mudring, *Phys. Status Solidi B*, 2013, **250**(6), 152.
48. Z. He, P. Alexandridis, *Phys. Chem. Chem. Phys.*, 2015, **17**, 18238.
49. T. Greaves and C. Drummond, *Chem. Soc. Rev.*, 2013, **42**, 1096.
50. C. Vollmer and C. Janiak, *Coord. Chem. Rev.*, 2011, **255**, 2039–2057.
51. T. L. Greaves and C. J. Drummond, *Chem. Soc. Rev.*, 2008, **37**, 1709–1726.

Graphical Abstract

Green solvents ionic liquids: structural directing pioneers for microwave assisted synthesis of controlled MgO nanostructures

Arvind H. Jadhav, Alan C. Lim, Gaurav M. Thorat, Harsharaj S. Jadhav, and
Jeong Gil Seo*

